Review

Two-Dimensional and Spheroid-Based Three-Dimensional Cell Culture Systems: Implications for Drug Discovery in Cancer

Anali del Milagro Bernabe Garnique [1], Natália Sudan Parducci [1], Lívia Bassani Lins de Miranda [1], Bruna Oliveira de Almeida [1], Leonardo Sanches [2] and João Agostinho Machado-Neto [1,*]

[1] Department of Pharmacology, Institute of Biomedical Sciences, University of São Paulo, São Paulo CEP 05508-900, Brazil; anabega@usp.br (A.d.M.B.G.); nataliasudanparducci@gmail.com (N.S.P.); liviamirands@usp.br (L.B.L.d.M.); bruolialmeida@usp.br (B.O.d.A.)
[2] Department of Biochemistry, Institute of Chemistry, University of São Paulo, São Paulo CEP 05508-900, Brazil; leonardo2.sanches@usp.br
* Correspondence: jamachadoneto@usp.br; Tel.: +55-11-3091-7467

Abstract: The monolayer (two-dimensional or 2D) cell culture, while widely used, lacks fidelity in replicating vital cell interactions seen in vivo, leading to a shift toward three-dimensional (3D) models. Although monolayers offer simplicity and cost-effectiveness, spheroids mimic cellular environments better. This is due to its nutrient gradients, which influence drug penetration and provide a more accurate reflection of clinical scenarios than monolayers. Consequently, 3D models are crucial in drug development, especially for anti-cancer therapeutics, enabling the screening of cell cycle inhibitors and combination therapies vital for heterogeneous tumor populations. Inhibiting processes like migration and invasion often require drugs targeting the cytoskeleton, which can exhibit dual functionality with cell cycle inhibitors. Therapeutic approaches with promising anti-cancer potential often exhibit reduced efficacy in 3D cell culture compared to their performance in monolayer settings, primarily due to the heightened complexity inherent in this system. In the face of this scenario, this review aims to survey existing knowledge on compounds utilized in both 2D and 3D cell cultures, assessing their responses across different culture types and discerning the implications for drug screening, particularly those impacting the cell cycle and cytoskeletal dynamics.

Keywords: cell cycle drugs; cytoskeleton drugs; monolayer; spheroids; 3D cell culture

1. Introduction

Monolayer studies are fundamental and widely recognized as the gold standard across numerous research domains, particularly in cancer research. Ross G. Harrison made pioneering contributions to cell culture techniques, notably introducing a groundbreaking method for culturing and observing living nerve fibers during embryonic frog development. Harrison's innovative approach involved placing a fragment of the spinal cord in lymph clot on a glass slide and sealing it with a cover slip [1].

Building on Harrison's work, Alexis Carrel developed various methodologies aimed at improving cell culture practices. He notably introduced the Carrel flask, known for its curved neck that facilitated culture medium exchange while preventing contamination [2]. Another significant advancement in cell culture came from Harry Eagle, who pioneered the development of suitable culture media for maintaining various cell lines [3,4].

By the 1950s, discussions in cellular biology symposia were already mentioning the use of cell culture as a system for studying drug activity [4], alongside its combination with other drugs that demonstrated improved cytotoxicity and collateral sensitivity [5]. One of the early pioneers in the large-scale screening of antineoplastic drugs using cell lines was Eagle and Foley (1958), establishing it as a modality still in use today [6].

Cell-based studies, notably in monolayer cultures, have greatly enhanced our grasp of chemotherapy's utility and deepened our understanding of tumor cell biology and

cellular processes. Traditional drug testing in these cultures offers a straightforward approach, allowing for direct interactions between drugs and cells without physical barriers. Insights gained from monolayer experiments shed light on cellular migration intricacies involving cytoskeletal structures, focal adhesion complexes, and various proteins [7]. While invaluable for exploring potential anti-cancer agents during initial compound development, it is essential to acknowledge the inherent limitations of monolayer cultures [8].

In contrast, in vivo therapy encounters a more intricate landscape, grappling with substantial hurdles in distributing drugs throughout tumors due to their three-dimensional (3D) structure and interactions with the surrounding stromal environment, altering drug diffusion profiles [9]. The evolution of chemotherapy studies has underscored disparities between in vitro drug behavior and in vivo settings, spotlighting the pivotal role of immune cells in cancer contexts [10]. As a result, there has been a pursuit for systems capable of faithfully replicating in vivo responses with high reproducibility. For certain cancer types, like endometrial cancer cells, monolayer cultures may inadequately mimic the presence of an appropriate extracellular matrix (ECM), impacting integrin signaling and downstream pathways such as PI3K/AKT, which regulate cellular proliferation mechanisms [11].

Tumor tissues exhibit complex 3D structures with physiological barriers that impede effective drug penetration. This presents a significant limitation in monolayer-based research, as it lacks fidelity to human physiological conditions [12]. Insights derived from three-dimensional (3D) cell culture systems are pivotal in comprehending the intricate tumor microenvironment, making them the preferred model for evaluating anti-tumor drug efficacy [11]. Figure 1 provides a schematic summary comparing monolayer and 3D characteristics.

Figure 1. Diagram illustrating the characteristics of monolayer cell culture models and 3D spheroids, highlighting the unique features of each system. Created with Biorender.com (accessed on 1 May 2024).

Malignant tumors, characterized by uncontrolled cell growth, typically stem from cell cycle dysregulation. This has led to extensive research efforts aimed at identifying molecular inhibitors targeting this pathway [13,14]. Our discussion will delve into the

continuous assessment of drugs in both monolayer and 3D systems, aiming to refine screening techniques for novel drug development. These advancements seek to improve in vivo response outcomes and are being evaluated across diverse cancer types, with a specific focus on their efficacy in monolayer cultures.

2. Drugs That Target the Cell Cycle in a Three-Dimensional Cell Culture (3D) System

The pursuit of a system mirroring in vivo conditions has driven the creation of diverse models, with 3D cell culture emerging as a prominent example. This review focuses on one particular type of 3D system: spheroids. Their significance lies in their ability to replicate the 3D architecture of solid tumors and emulate the intricate cell–cell and cell–matrix interactions observed in vivo [15]. Currently, a wide variety of techniques are available for spheroid generation, such as scaffold-based culture (hydrogel or other polymeric materials) and scaffold-free culture (using magnetic levitation, hanging-drop microplates, and non-adherent coated microplates) [16].

The spheroids can recapitulate three important regions: an outermost proliferative zone with higher nutrient and oxygen concentration, followed by a layer of quiescent cells, and, further toward the center, a cluster of necrotic cells. As the layers internalize, higher concentrations of cellular debris and carbon dioxide are found due to the low concentrations of oxygen and nutrients [17]. The development of these gradients is only observed in spheroids with diameters between 200 and 500 μm [18]. This characteristic generates a protective effect on the innermost cells of the spheroid, already subjected to stressful conditions and partially shielded, in certain cases, from the impact of drugs retained in the outer layers, as was demonstrated in the study with temozolomide in glioblastoma cell lines [19].

Cell culture models exhibit variations in morphology, signal transduction, histone acetylation, gene expression, protein expression, drug metabolism, proliferation zones, viability, hypoxia, pH, differentiation, migration, and drug sensitivity [20]. Several studies comparing drug testing in 2D and 3D systems of the same cell line have noted dissimilar dose–response curves, with 3D models displaying increased resistance to treatments. To illustrate, we provide a concise summary of drugs used in monolayers (Table 1) and discuss select drugs employed in 3D settings [21,22].

The treatment with 5-fluorouracil induced less cell death in spheroids of the HepG2 (hepatocarcinoma) cell line than in monolayers due to increased intercellular adhesion through E-cadherin and CD44v6, resistance due to differentiated phenotypes, and greater tolerance to stressful stimuli [22–26]. The inhibitory concentration of 50% (IC$_{50}$) for MCF-7 (breast cancer) spheroids showed an approximate 2.24-fold increase compared to the monolayer culture upon arsenic administration [23]. Studies with binimetinib [24], docetaxel [21], and romidepsin [22] serve as other examples of increased resistance in 3D cell culture systems. An overview of monolayer cell culture drugs targeting the cell cycle is described in Table 1. Studies conducted on spheroids with the drugs and concentrations used in them are described in Table 2.

Table 1. Cell cycle and cytoskeleton targeting drugs and their mechanism of action, main indications, and in vitro inhibitory concentration of 50% (IC$_{50}$).

Category	Drug	Mechanism of Action	Main Indications	In Vitro IC$_{50}$
Cyclin-dependent kinase (CDK) inhibitors	Palbociclib	Suppression of RB1 phosphorylation during the G$_1$ to S phase transition.	Advanced breast cancer, metastatic breast cancer, and refractory breast cancer.	30–89 μM *
	Ribociclib	Selective inhibition of CDK4/6, resulting in reduced phosphorylation of RB1.	Advanced breast cancer and metastatic breast cancer.	0.5–1109.6 μM **
	Abemaciclib	Inhibition of CDK4/6, resulting in cell cycle disruption and induction of G$_1$ phase arrest.	Advanced breast cancer and metastatic breast cancer.	0.05–2.7 μM *

Table 1. *Cont.*

Category	Drug	Mechanism of Action	Main Indications	In Vitro IC$_{50}$
Tyrosine kinase inhibitors	Crizotinib	Inhibition of ALK, ROS1, and MET, leading to reduced cell proliferation, suppressed migration, G$_1$ cell cycle arrest, apoptosis, and increased chemotherapy resistance.	Metastatic non-small cell lung cancer.	0.01–2.2 µM *
	Ibrutinib	Irreversible inhibition of BTK.	Chronic lymphocytic leukemia, mantle cell lymphoma, and Waldenstrom's macroglobulinemia (EM).	0.58–2.5 µM *
	Imatinib	Inhibition of ABL1, BCR::ABL1, PDGFR-α and -β, and KIT.	Chronic myeloid leukemia and multiple cancer types.	0.07–100 µM *
	Erlotinib	Inhibition of EGFR kinase domain.	Locally advanced non-small cell lung cancer, locally advanced pancreatic cancer, metastatic non-small cell lung cancer, non-small cell lung carcinoma, and metastatic pancreatic cancer.	0.0437–199 µM **
	Gefitinib	Inhibition of EGFR kinase domain.	Metastatic non-small cell lung cancer, colorectal cancer, and breast cancer.	0.0648–805 µM **
	Dasatinib	Inhibition of BCR::ABL1, KIT, and other targets.	Acute lymphoblastic leukemias and chronic myeloid leukemia.	0.00106–92 µM **
	Axitinib	Inhibition of VEGFR1, VEGFR2, and VEGFR3.	Renal cell carcinoma, hepatocellular carcinoma, progressive differentiated thyroid cancer and advanced thyroid cancer.	0.7–12.5 µM *
	Nilotinib	Inhibition of KIT and PDGF receptors. Gastrointestinal stromal tumors, and breast cancer resistant to endocrine therapies.	Chronic myeloid leukemia, gastrointestinal stromal tumors, and breast cancer resistant to endocrine therapies.	0.002–1272.78 µM **
	Osimertinib	Selective inhibition of EGFR mutations.	Metastatic non-small cell lung cancer.	0.002–14.9 µM *
	Sorafenib	Inhibition of VEGFR1, VEGFR2, and VEGFR3.	Advanced renal cell carcinoma, hepatocellular carcinoma, progressive differentiated thyroid cancer, and multiple cancer types.	0.00428–168 µM **
	Regorafenib	Inhibition of multiple kinases.	Gastrointestinal stromal tumor, osteosarcoma, and colorectal cancer.	1.3–82.4 µM *
Histone Deacetylase (HDAC) Inhibitors	Panobinostat	Inhibition of HDACs.	Refractory multiple myeloma.	0.001–29 µM **
	Vorinostat	Inhibition of HDACs.	Persistent cutaneous T-cell lymphoma, progressive cutaneous T-cell lymphoma, and recurrent cutaneous T-cell lymphoma.	0.99 nM–49.8 µM *
Platinum-Based Anticancer Drugs	Cisplatin	Formation of Pt-DNA, inducing double-strand breaks in DNA, leading to cell death.	Multiple cancer types.	0.177–10198.4 µM **
	Oxaliplatin	Inhibition of processes related to DNA replication and transcription, leading to cell cycle arrest and cell death.	Multiple cancer types.	1.04–35.6 µM *

Table 1. *Cont.*

Category	Drug	Mechanism of Action	Main Indications	In Vitro IC$_{50}$
Anthracyclines	Doxorubicin	DNA intercalation and topoisomerase II inhibition, inducing oxidative stress and apoptosis.	Multiple cancer types.	0.00454–38.8 μM **
	Epirubicin	Inhibition of DNA transcription and RNA synthesis.	Breast, liver, gastric, and non-small cell lung cancer.	0.02–9.9 μM *
	Etoposide	Stabilization of the enzyme–DNA complex and induction of permanent DNA strand breaks, leading to cell death.	Multiple cancer types.	0.12–241.9 μM *
	Gemcitabine	Incorporation of fluorinated nucleotide analogs into DNA, inhibiting nuclear replication.	Multiple cancer types.	0.000628–50.6 μM **
	5-Fluorouracil	Inhibition of thymidylate synthase and substitution of nucleotides in DNA, interrupting DNA replication and repair.	Breast cancer, malignant neoplasm of colon, malignant neoplasm of pancreas, malignant neoplasm of stomach, rectal carcinoma, superficial basal cell carcinoma, and others.	0.3–47.9 μM *
Topoisomerase Inhibitors	Topotecan	Inhibition of topoisomerase I, inducing DNA strand breaks.	Acute myeloid leukemia, Ewings sarcoma, refractory neuroblastoma, metastatic rhabdomyosarcoma, cervical cancer; refractory central nervous system lymphoma, refractory central nervous system malignancy, refractory or metastatic ovarian cancer, and relapsed small cell lung cancer.	0.005 7–339 μM **
DNA Alkylators	Temozolomide	Alkylation of genomic DNA, inducing nucleotide mismatches and triggering cell cycle arrest in the G$_2$/M phase, leading to cancer cell death.	Advanced melanoma, glioblastomas, primary central nervous system lymphoma, refractory Ewing sarcoma, refractory neuroblastoma, soft tissue sarcoma, advanced neuroendocrine tumor, refractory anaplastic astrocytoma, refractory, advanced mycosis fungoides, and refractory or advanced Sezary syndrome.	4.34–766.1 μM *
	Trabectedin	Inhibition of activated transcription and cell cycle arrest in the S phase and G$_2$ phase.	Metastatic leiomyosarcoma, metastatic liposarcoma, relapsed platinum-sensitive ovarian cancer, unresectable leiomyosarcoma, and unresectable liposarcoma.	0.1–3.7 nM *

* https://www.selleckchem.com (accessed on 15 April 2024). ** https://www.cancerrxgene.org (accessed on 15 April 2024).

Table 2. Cell cycle and cytoskeleton targeting drugs used in spheroid studies.

Category	Drug	Type of Cancer	Used Concentration	Ref.
Cyclin-dependent kinase (CDK) inhibitors	Palbociclib	Glioblastoma	10 nM–10 μM	[25]
	Ribociclib	Pancreas cancer	0.16–100 μM	[26]
	Abemaciclib	Glioblastoma	10 nM–10 μM	[25]
Tyrosine kinase inhibitors	Crizotinib	Colon adenocarcinoma	250–500 nM	[27]
	Crizotinib	Lung cancer	2–5 μM	[28]
	Crizotinib	Gastric cancer	0.01–1 μM	[29]
	Ibrutinib	Hepatocellular carcinoma	2–6 μM	[30]

Table 2. *Cont.*

Category	Drug	Type of Cancer	Used Concentration	Ref.
Tyrosine kinase inhibitors	Imatinib	Glioblastoma	10 μM	[31]
	Imatinib	Adrenocortical carcinoma	10 μM	[32]
	Erlotinib	Lung cancer	2–10 μM	[28]
	Erlotinib	Colorectal carcinoma	0.6–5.5 μM	[33]
	Gefitinib	Lung cancer	>1 μM	[34]
	Dasatinib	Glioblastoma	IC_{50}: 42 μM	[35]
	Dasatinib	Prostata adenocarcinoma	IC_{50}: 102 μM	[35]
	Axitinib	Breast cancer	0.012–100 μM	[36]
	Osimertinib	Lung cancer	IC_{50}: 240 nM	[34]
	Sorafenib	Hepatocellular carcinoma	2–15 μM	[30,37]
	Regorafenib	Hepatocellular carcinoma	2.5–5 μM	[38]
	Regorafenib	Colon cancer	IC_{50}: 49.8 μM	[39]
	Regorafenib	Colorectal carcinoma	3.3–14.8 μM	[33]
Histone Deacetylase (HDAC) inhibitors	Vorinostat	Colon carcinoma	0.9 μM	[40]
	Vorinostat	Cervical cancer	200 nM	[41]
	Vorinostat	Glioblastoma	0.1–10 μM	[42]
Platinum-based anticancer drugs	Cisplatin	Lung cancer	IC_{50}: 66–126 μM	[43]
	Cisplatin	Cervical cancer	10 μM	[44]
	Cisplatin	Ovarian cancer	5–10 μg/mL	[45]
	Cisplatin	Lung cancer	78.6–>250 μM	[46]
	Cisplatin	Cervical cancer	21.4–250 μM	[46]
	Cisplatin	Osteosarcoma	17.4–122 μM	[46]
	Cisplatin	Glioblastoma	15.6–23.5 μM	[46]
	Cisplatin	Pancreatic cancer	4.57 μM	[47]
	Oxaliplatin	Colorectal cancer	0.1–100 μM	[48]
Taxane	Paclitaxel	Colorectal cancer	40 μM	[49]
	Paclitaxel	Ovarian cancer	40 μM	[49]
	Paclitaxel	Pancreatic cancer	IC_{50}: >80 nM	[47]
DNA damaging drugs	Doxorubicin	Ovarian cancer	0.2–2 μM	[50]
	Doxorubicin	Colorectal cancer	100 μM	[49]
	Gemcitabine	Lung cancer	87–177 μM	[43]
	Gemcitabine	Pancreatic cancer	28.17 μM	[47]
	5-Fluorouracil	Lung cancer	99–148 μM	[43]
	5-Fluorouracil	Colorectal carcinoma	1.4–9.2 μM	[33]
	Topotecan	Colorectal	1 nM–10 μM	[51]
	Temozolomide	Adrenocortical carcinoma	1–100 μM	[52]
	Temozolomide	Glioblastoma multiforme	100–300 μM	[53]

Although the term "spheroid" is widely used, Weiswald, Bellet, and Dangles-Marie [54] segregate them into multicellular tumor spheroid models, formed by two or more distinct cell lines; tumorsphere, with a single cell line; and tumor-derived spheroid, made of a primary culture of tumor cells. The resistance of these models to cancer treatments is a known event and it is justified based on the induction of stress response proteins in hypoxic regions and the multiple exposure to drugs, leading to a change in cell growth properties [55]. Assays conducted with oxaliplatin in HCT15, HCT116, and HCT116oxR cell lines (oxaliplatin-resistant colorectal cancer cell lines) revealed a significant reduction in cell cytotoxicity under hypoxic conditions in 3D compared to monolayer cultures, with the compound being 13 to 64 times less active in spheroids [56]. Fiorillo, Sotgia, and Lisanti [57] discovered a metabolic shift during the transition from anchorage-dependent to anchorage-independent growth, emphasizing the reliance of spheroid cell propagation on mitochondrial oxidative phosphorylation. This highlights the importance of developing drugs that inhibit this activity, as noted by other authors [58,59]. Despite higher drug concentrations often required for spheroid treatment, certain drugs exhibit similar effects in reducing cell proliferation and increasing rates of apoptosis, DNA damage, and reactive oxygen species generation, as demonstrated across both monolayer and 3D models, with olaparib applied to MDA-MB-231 (breast cancer), HCC1937 (breast cancer), and IGROV-1 (ovarian cancer) cell lines [60].

Assessing the effectiveness of drugs in spheroids requires considering their regionalization and heterogeneity, with a focus on drug penetrability in the structure. Laurent et al. [61] proposed analyzing the response of pancreatic cancer cells (Capan-2) to etoposide treatment, which demonstrated efficacy by penetrating the spheroid and inducing global changes in cell cycle distribution in its outer layers. Similarly, treatments with vincristine in EMT6/Ca/VJAC (breast cancer) cells underscore the heightened sensitivity of peripheral

cells to pharmacological effects due to their increased drug exposure and lower resistance to stress [62].

Treatment with imatinib induced the formation of gaps within Ishikawa (endometrial cancer) spheroids, resulting in diminished intercellular interactions, increased apoptosis, and induction of mitochondrial damage [58]. Additionally, compounds that hinder cell clustering and migration rates can lead to the deconstruction of spheroid structures, thereby reducing metastatic potential [63]. Notably, this effect was observed with Tamoxifen in NR-MCF-7 and TR-MCF-7 cell lines [64], as well as with Interferon (IFNβ) in A375 and SB2 (cutaneous melanoma) cell lines [63]. In another study comparing adrenocortical carcinoma cells treated with drugs like imatinib, sunitinib, zoledronic acid, among others, researchers observed that spheroids formed by these cells showed increased resistance compared to those in monolayer cultures. This finding highlights how spheroid formation correlates with reduced sensitivity to chemotherapy, mirroring observations in actual tumors [32].

Another parameter used to measure the potency of drugs in a 3D system is their volume. The reduction in spheroid size often indicates the drug's ability to overcome cellular aggregation barriers and penetrate the tumor structure. This phenomenon has been observed with abemaciclib [65], cisplatin [66], methotrexate [67], and erlotinib [68]. Furthermore, the anticancer activity of these drugs was linked to increased percentages of apoptotic cells and inhibition of autophagy, suggesting potential enhancement with combined drug therapies [28]. The study conducted on glioblastoma and prostate cells compared the effects of monolayer culture versus spheroids and bioprinting when treated with the drug dasatinib. It showed similar responses between bioprinting and spheroids, likely due to the challenges in drug penetration observed in 3D cultures. Additionally, the study underscored the importance of characteristics like feasibility, reproducibility, and scalability to ensure consistency across 3D cultures [35].

In line with findings from monolayer studies, specific drugs targeting cell cycle components are employed in 3D cell culture research. G_2/M arrest is a mechanism widely exploited by the pharmaceutical industry to prevent cell division. The literature shows its application and efficiency in 3D model of prostate cancer (axitinib) [69], lung cancer (cabazitaxel) [70], colorectal cancer (docetaxel) [71], and breast cancer (epirubicin and hyaluronidase) [72,73]. A similar effect was observed in treatments with rucaparib in PC3 and LNCaP (prostate cancer) cell lines, delaying spheroid growth by increasing the rate of cell death [74]. Other studies reported a G_1/S phase arrest, such as the application of selinexor in gastric cancer cells, especially when combined with paclitaxel [75]. Treatment with 5 μM of temsirolimus also slowed the growth of H1 and H3 spheroids in melanoma [76].

In addition to testing isolated drugs, there are assays dedicated to analyzing the synergistic effects between drugs, a scenario that maximizes the benefits of using spheroids. For example, the combination of cisplatin with MK-1775 reduced the volume of human bladder epithelium spheroids by up to 80% in animals treated with 1 μM Cisplatin and 0.2 μM MK-1775 [66], highlighting the potential of synergy studies to enhance the efficacy of combination treatments by leveraging the individual effects of each drug. Other combinations include bortezomib (10 nmol/L) and TMZ (200 μmol/L) for glioma treatment, tested with U251 and U87 cell lines [77]; carfilzomib and flavopiridol for adrenocortical carcinoma monolayer—NCI-H295R (IC_{50} = 0.13 μM and 0.02 μM, respectively) and SW-13 (IC_{50} = 0.42 μM and 0.42 μM) cell lines [78]; dasatinib and salinomycin for breast cancer—MDA-MB-468 (IC_{50} Sal/Das in monolayer = 0.5 and 15 μM; IC_{50} Sal/Das in spheroids = 4 and 30 μM), MDA-MB-231 (IC_{50} Sal/Das in monolayer = 0.1 and 0.2 μM; IC_{50} Sal/Das in spheroids = 8 and 1.1 μM), and MCF-7 (IC_{50} Sal/Das in monolayer = 6.5 and 12 μM; IC_{50} Sal/Das in spheroids = 25 and 48 μM) cell lines [79]; Gemcitabine and gefitinib for esophageal cancer—KYSE-270 (ED_{95} = 0.59), KYSE-410 (ED_{95} = 0.58), and KYSE-520 (ED_{95} = 0.43) cell lines [80]; and Medroxyprogesterone and imatinib for Ishikawa cell line (IC_{50} = 200 and 50 μM) [58]. The growth inhibition mechanisms in synergism tests are like those found in isolated treatments, with emphasis on G_2/M phase arrest [78,80],

stimulation of caspase activation [81], and induction of reactive oxygen species (ROS) formation [79].

The advantages of synergism are evident in various scenarios, such as the treatment of lung cancer cell lines (H460 and A549) with paclitaxel, cisplatin, irinotecan, and etoposide, resulting in reduced viability, migration, and invasion, particularly in H460 spheroids [82]. Combinations can also be strategically planned to delay resistance to compounds, as demonstrated by La Monica and colleagues [65]. Their study showed that the combined use of osimertinib and abemaciclib prevented or delayed resistance to osimertinib treatment in lung cancer cell lines (PC9 and HCC827), reducing the number of colonies formed.

Turning to protein expression, drugs have been increasingly refined by the precise selection of proteins that modulate the growth and survival of cells in 3D. Carboplatin (100–150 µmol/L), used in the treatment of ovarian cancer, promotes the inhibition of DYRK1A, thereby increasing the rate of cell death in OVCAR3, OVCAR5, and OVCAR8 (ovarian cancer) spheroids [83]. Similarly, gefitinib also induced cell death, along with S phase arrest by cyclin D1 [80], and doxorubicin reduced cell invasion, as demonstrated in choriocarcinoma cell lines [84].

Among the proteins receiving particular attention is MEK, a kinase within the RAS/ RAF/MEK/ERK cascade responsible for mediating cellular responses to various growth factors [85]. Reduced expression of MEK, induced by vorinostat in combination with selumetinib, inhibited the formation of colon cancer spheroids [86]. Trametinib, administered at concentrations of 10 nM and 100 nM, also decreased the proportion of proliferative cells in 3D cell cultures of ID8-KRAS (ovarian cancer) by inhibiting the RAS/RAF/MAPK pathway, without affecting 2D cell cultures of the same lineage [87].

Other proteins studied recently using the spheroids include PTK6 (regulator of survival, cell cycle, and cell differentiation), with reduced expression in PC3, DU145, and LNCaP (prostate cancer) cell lines when treated with ibrutinib [88]. Cadherin (adhesion formation), inhibited by Nab-paclitaxel in MIA PaCa-2, PANC-1, and AsPC-1 (pancreatic cancer) cell cultures [89]; and histone deacetylases (interfering with survival, cell cycle, and differentiation) with reduced activity in sarcoma cells (DTC1, KAO, and SU-CCS-1) by romidepsin [90]. Genes involved in cell cycle arrest and protein ubiquitination also had increased regulation with the treatment of 5 µM topotecan in ovarian cancer spheroids (OV-CAR3, SKOV3, TOV-112, TOV-21, and OV-90), while others associated with biosynthesis, immune responses, inflammation, and molecular transport had decreased expression [91].

In summary, despite a considerable number of publications aimed at testing treatments in monolayer cell culture, 3D systems are becoming more advantageous, as they more accurately simulate the action and effectiveness of compounds when applied to in vivo models.

3. Drugs That Target the Cytoskeleton in 2D and 3D Cell Culture

The cytoskeleton, a dynamic network of polymerized proteins, is crucial for cell division, maintaining shape, and facilitating motility by organizing cellular contents and enabling interaction with the environment. Comprising microtubules, actin filaments, and intermediate filaments, this structure coordinates various cellular processes through precise assembly and disassembly [92,93]. The cytoskeleton is composed of three types of molecules that form different polymers: microtubules, actin filaments, and intermediate filaments, and each of these presents different structures and, therefore, participates in specific functions [94].

Microtubules, one of the primary cytoskeletal proteins, are vital for cell division, forming the mitotic spindle that aligns and separates chromosomes during mitosis. Their dynamic nature enables this process [93]. Actin filaments, meanwhile, facilitate cell-to-cell communication and migration by forming polymer networks and supporting filopodial protrusions [95]. Intermediate filaments contribute to the cell's resistance to mechanical stress [96]. Given their importance, there is significant interest in developing anti-neoplastic drugs targeting the cytoskeleton. Traditional agents targeting the cytoskeleton, particularly

microtubules, function as antimitotic agents by interfering with cell cycle progression [97]. Microtubule-stabilizing drugs promote tubulin polymerization, leading to mitotic blockade and apoptosis [98]. Examples include taxols, epothilones, and marine-derived compounds like discodermolide. Microtubule-destabilizing agents, like vinca alkaloids and colchicine analogs, also exhibit antimitotic effects [99,100].

Actin cytoskeleton-targeting agents inhibit cell motility, making them effective against metastasis [101]. However, addressing metastasis presents challenges due to its complexity and potential toxicity, necessitating careful clinical application. Nonetheless, research into anti-migrational drugs, especially those targeting microfilaments, has surged. Many of these studies focus on natural compounds, as anti-invasive mechanisms may mirror defense strategies observed in various terrestrial and marine organisms [101].

Like tubulin-targeted agents, drugs that impact actin filaments are classified as either destabilizers or stabilizers. Recent research has shed light on the complex nature of actin polymerization, involving not only actin molecules binding to each other but also a continuous competition among various proteins for binding sites on actin. Consequently, agents targeting actin also compete for these binding sites [102]. Nevertheless, the previous classification remains valid. Some compounds described as stabilizers of the actin cytoskeleton, such as jasplakinolide and chondramides, which compete with phalloidin for the F-actin binding site, and cucurbitacin E, an inhibitor of actin depolymerization, can initially be tested in monolayer cultures [101,103,104]. Within the class of actin cytoskeleton destabilizers, notable examples include the extensively studied cytochalasin and latrunculin, both of which inhibit actin polymerization. Additionally, geodiamolides are recognized as disruptors of actin filaments [77,79–81].

It has been observed that approved drugs spanning various classes and targets may also influence cytoskeletal proteins or regulate cytoskeleton dynamics by interacting with other proteins. An example of this is doxorubicin, an antibiotic belonging to the anthracycline group derived from *Streptomyces peucetius*. Doxorubicin has been utilized as a chemotherapeutic agent to combat a diverse array of tumors [105]. Studies show that nanoparticle formulations with doxorubicin can affect cytoskeleton dynamics. Nanoparticles synthesized by incorporating doxorubicin, curcumin, and perfluorooctyl bromide into poly (lactic-co-glycolic acid) inhibited polymerization of the actin cytoskeleton in the MCF-7 cell line [106]. Proteomics and further bioinformatics analysis revealed that doxorubicin-CaCO3-nanoparticles modulate the expression of several structural proteins including α/β-tubulin and actin in MCF-7 cells, indicating that the system may induce regulation of migration and endocytosis in this cell line [107]. Lastly, changes in the actin cytoskeleton in A549 cells were observed using time-lapse imaging and transwell assays when cinnamic acid derivatives were co-administered with doxorubicin [108]. Epirubicin is an anthracycline epimer of doxorubicin that has also been used as a cytotoxic drug against a variety of tumors. Migration assays, such as wound-healing and Boyden chamber assays, revealed that treating MDA-MB-231 cells with a low dose of epirubicin resulted in inhibited migration. Additionally, a decrease in the expression of ezrin, a protein from the ERM family that participates in the linking of the actin cytoskeleton to the cell membrane, was observed [109,110]. These studies contribute to a deeper understanding of chemotherapy drugs' impact on cellular processes beyond their primary mechanisms of action, offering insight into future drug development and combined strategies of treatments.

Other drugs can modify cell morphology and other cellular process like methotrexate, which is an antimetabolite of folic acid that inhibits the synthesis of purines and pyrimidines, disrupting synthesis, repair, and replication of the DNA strands, and ultimately leading to cell division blockage [111]. A study utilizing CaSki cells, a cervical cancer cell line, and NRK, normal fibroblasts, showed that methotrexate treatments cause the cells to shrink. The exposure to the drug caused the redistribution of G-actin toward the nucleus for CaSki cells and disassembly of F-actin on NRK models, increasing lamellipodial activity for both cell lines [111,112].

Cisplatin is a well-known drug utilized to treat numerous types of neoplasms. The literature indicates that treatments with Cisplatin in MCF-7 and MDA-MB-231 cell lines induce the expression of ATF3, which encodes a protein member of the CREB family [113], and that it suppresses the activation of FN1, a gene that encodes for fibronectin, a protein that participates in cell migration, adhesion, and differentiation [114]. This study indicates that the modulation compromises epithelial-to-mesenchymal transition (EMT) and cell migration [115].

A study utilizing HeLa (cervical cancer) and U2OS (osteosarcoma) cells indicated that treatments with topotecan affected the microtubule cytoskeleton and inhibited actin polymerization, interfering not only with cell cycle progression but also reducing the mass of actin filaments [116]. Additionally, another study analyzing the effects of topotecan in cell migration revealed that the treatments regulated the expression of E-cadherin, N-cadherin, and vimentin, resulting in the suppression of the EMT phenotype in H1299, H1975, and HCC827 lung cancer cells [117,118]. Thus, these studies demonstrate that drugs targeting the cytoskeleton influence proteins involved in EMT, a critical process in the development of invasion and metastasis to other organs.

Drugs such as tyrosine kinase inhibitors can impact cellular protrusions like filopodia, which play a crucial role in cell migration and communication, potentially inhibiting the spread and invasive behavior of cancer cells. Various kinase inhibitors have been identified to disrupt components of the cytoskeleton, offering targeted therapy for different neoplasms characterized by specific mutations in proteins catalyzing the transfer of ATP's terminal phosphate to serine, threonine, or tyrosine residues [119]. The groundbreaking kinase inhibitor, imatinib, significantly improved disease outcomes for chronic myeloid leukemia patients [120]. In a study using the LS180 colorectal cancer cell line, treatment with imatinib induced cells to adopt a rounder shape compared to untreated cells, accompanied by long, finger-like protrusions. At higher drug concentrations, actin filaments began to aggregate, leading to a decrease in total actin polymerization [121].

EGFR inhibitors are commonly employed in the treatment of non-small-cell lung cancer, including first-generation drugs like gefitinib and erlotinib, as well as the third-generation drug osimertinib [122]. These drugs have demonstrated interference with cytoskeleton structures. In a study using OE21 and OE33 cell lines, treatment with gefitinib and erlotinib resulted in alterations in cell morphology and the actin cytoskeleton, leading to a decrease in the number of filopodia and microspikes. Molecular assays indicated that these tyrosine kinase inhibitors interfered with RhoGTPase and FAK activity [123]. In another study involving modified lung carcinoma cell lines (PC-9 L861Q+19del and PC-9 L861Q), researchers observed that treatment with gefitinib, erlotinib, and osimertinib led to a reduction in cell size. Furthermore, these inhibitors altered the distribution of microfilaments, resulting in nuclear fragmentation, a phenomenon associated with apoptosis [124]. Other studies have compared the use of erlotinib in 2D versus 3D culture in lung cancer cells, finding that treatment with erlotinib induces caspase 8 activation and upregulation of TNF-related apoptosis-inducing ligand (TRAIL) solely in 3D culture. It also modulates autophagy markers and activates JNK. This suggests that Erlotinib induces apoptotic cell death in 3D cultures through an autophagy-TRAIL-JNK pathway, thus aiding in better elucidating the mechanism of this drug [125].

Histone deacetylase inhibitors (HDACis) represent a class of targeted therapy known for their role in altering gene transcription and chromatin remodeling. Histone deacetylases (HDAC) catalyze the removal of acetyl groups from histone and nonhistone proteins, influencing transcription regulation [126]. Examples of HDAC inhibitors include panobinostat and vorinostat. In a study involving human megakaryocyte cells treated with panobinostat, researchers observed an increase in tubulin polymerization and structural alterations in microtubule dynamics [127]. Additionally, another study with U87-MG glioma cells found that vorinostat, at low concentrations, induced tubulin detyrosination and tubulin acetylation, impacting microtubule dynamics [128].

In 3D contexts, the cytoskeleton's involvement in spheroid formation is pivotal, as it facilitates interactions between various proteins and the extracellular matrix. Spheroid assembly typically progresses through three stages. It initiates when cells are incapable of attaching to a surface aggregate, prompted by their proximity. This prompts an increase in cadherin expression due to cell-to-cell contact. Cadherin accumulates in cell membranes, fostering the formation of compact structures via homophilic binding between adjacent cadherin molecules [104–106].

Integrins also play a crucial role in the spheroid assembly process, and their activation is associated with focal adhesion kinase (FAK) activity [128]. FAK is a protein pivotal in cell adhesion, migration, and growth. It transmits extracellular signals mediated by integrins and contributes to the rearrangement of actin filaments and microtubules [129]. Studies indicate that the actin cytoskeleton reinforces cell–cell contacts during spheroid formation, while microtubules are involved in the compaction and growth phases of assembly. Together, these proteins contribute to stabilizing the spheroid structure [104,107].

Studies investigating the effects of compounds targeting the cytoskeleton in spheroid cultures can be limited. L'Espérance et al. described the effects of cisplatin, paclitaxel, and topotecan on gene expression in ovarian carcinoma spheroids. The results revealed that cisplatin treatments led to a general downregulation of genes related to cytoskeletal structure and cell adhesion. On the other hand, exposure to paclitaxel increased the expression of these genes, whereas treatment with topotecan elicited both upregulation and downregulation responses within the spheroids [91]. The observed downregulation in the study may be attributed to the interplay between cellular adhesion stability and cytoskeletal integrity in the spheroid system [130]. Conversely, exposure to cisplatin and topotecan led to increased expression of genes associated with cell adhesion and the cytoskeleton, possibly reflecting the spheroid's adaptive response to these treatments [91].

It has been noted that various cancer cell lines respond differently to the same chemotherapy drug, such as cisplatin, which demonstrates limited effectiveness against certain osteosarcoma cell lines. Using a diverse panel of cell lines, spheroids were formed and exposed to cisplatin. The delayed cytotoxic response observed in 3D cultures suggests the involvement of endocytosis and intracellular trafficking. Although ATP generation was promptly inhibited, reflecting rapid cisplatin effectiveness, changes in ATP production indicated alterations in cell morphology and movement, suggestive of cell–extracellular matrix interactions. Interestingly, while most cell lines exhibited a swift decline in ATP generation post-treatment, some spheroids maintained ATP production, hinting at potential resistance or rapid metabolic clearance of cisplatin in these cells [46].

The possibility of drug combinations and their delivery has enabled the investigation of drug penetration. In this study, NCI/ADR-RES cells (ovarian cancer) were used to form spheroids and test drug combinations, doxorubicin delivery, different formulations, as well as timing and their influence on cytotoxicity. This study suggests that spheroid models are effective for assessing drug combinations and schedules, with findings aligning with clinical and in vitro studies. The results also highlight the potential for using these models to test tumor-targeted drug formulations [49].

While monolayer cultures offer a clearer visualization and characterization of drug effects on the cellular cytoskeleton, providing insight into morphological changes at the single-cell level, research on spheroids in 3D contexts remains notably scarce. This could be attributed to the inherent complexity of spheroids. Most studies focus on the drug's impact on a general population, often evaluating cytotoxicity levels. However, in 3D culture models, such as spheroids, the cytoskeleton's role in drug response becomes evident, with some drugs facing challenges in penetrating these structures, leading to delayed cytotoxic responses and potential drug resistance. Thus, spheroid models have emerged as valuable tools for assessing these strategies, offering insights that align with clinical and in vitro studies. A summary of the molecular pathways targeted by drugs that focus on the cell cycle and the cytoskeleton is described in Figure 2.
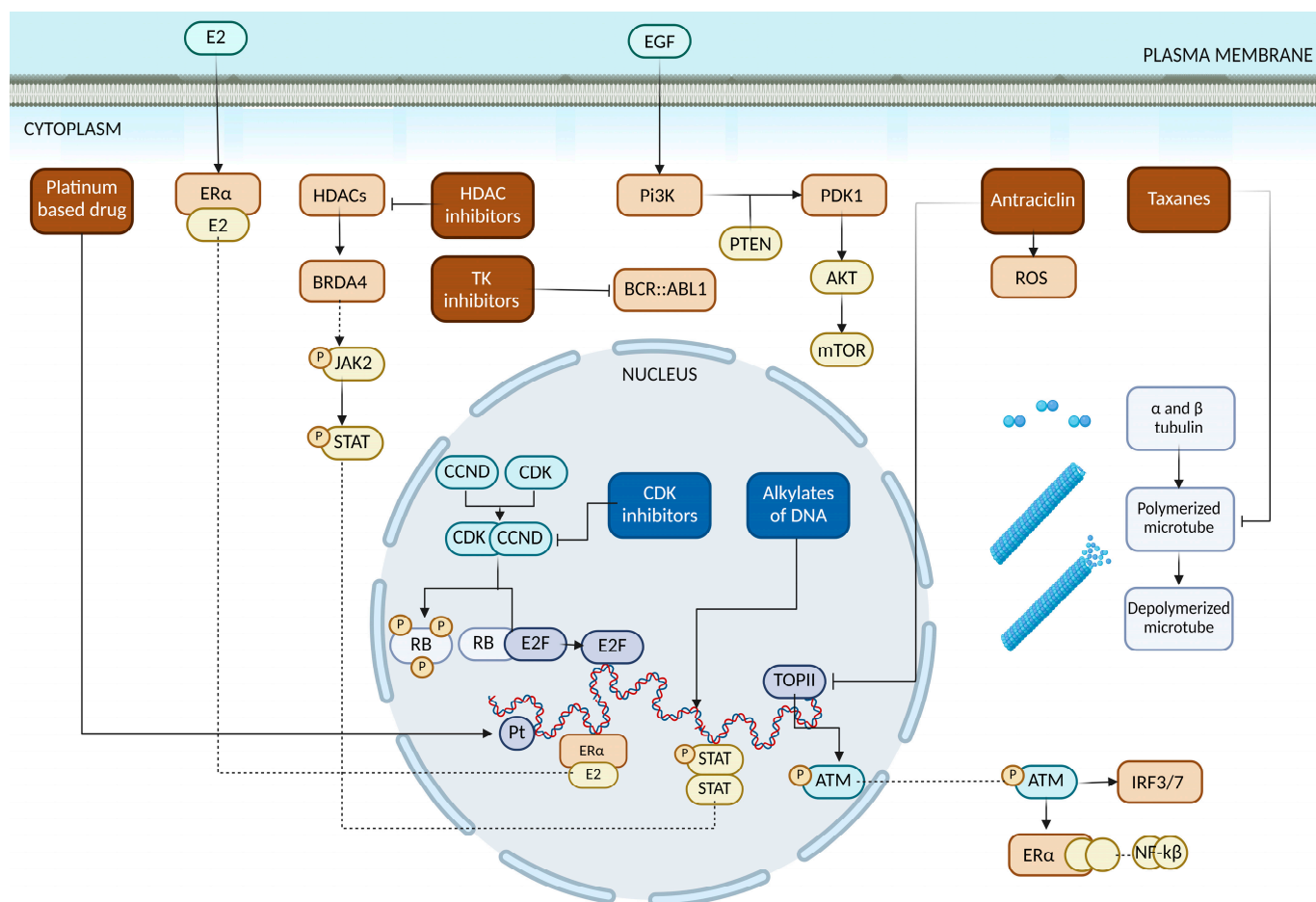
Figure 2. Summary of the molecular pathways targeted by drugs that focus on the cell cycle and the cytoskeleton. Created with Biorender.com (accessed on 1 May 2024).

4. Enhancing Drug Screening in 3D Cell Cultures

In 3D cell cultures, aggregates or spheroids can be formed using scaffold-based or scaffold-free methods. The intricate interplay between matrices and scaffolds shapes cell behavior, aiming to mimic in vivo conditions. These scaffolds, made from natural and synthetic polymers, replicate the extracellular matrix, enhancing cell interactions and expression [131]. For drug screening, methodological differences may influence drug response due to variations in spheroid formation and population dynamics, reminding us that standardization and homogeneity in 3D cultures are crucial for reliable drug testing.

Additionally, bioengineering approaches, like co-cultures, mimic physiological environments, optimizing cell function and tissue engineering by creating constructs with heterotypic cellular interactions vital for cancer progression. A study generated a 3D human breast cancer model by co-culturing cancer cells and fibroblasts in a rotating suspension culture system, showing cancer cell invasion into fibroblast spheroids and protein expression similar to breast cancer tissue [132]. A photocrosslinkable chitosan was used to fabricate hydrogel microstructures that transitioned from cell-repellent to cell-adhesive, enabling patterned co-cultures of spheroids and support cells. This system is useful for studying heterotypic cell–cell interactions, drug screening, and developing implantable bioartificial organs [133]. The study on NSCLC cells reveals correlations between EMT and spheroid generation efficiency. Advanced IMC analysis unveils spatial organization and marker expression in epithelial and mesenchymal-like cancer cells, and their interactions with fibroblasts. Deep-learning-based segmentation enables multiparametric analysis, highlighting EMT marker heterogeneity. These findings advance NSCLC drug screening strategies [134]. In 3D heterotypic spheroid models, senescent fibroblasts induced prolifera-

tion and nuclear atypia in OSE cells, highlighting the potential of 3D heterotypic modeling in understanding ovarian cancer etiology [135].

Thus, 3D models can simulate complex diseases like cancer, fibrosis, and neurodegenerative disorders, facilitating the study of disease progression and the identification of new therapeutic targets. They also allow researchers to observe dynamic processes such as tumor growth, angiogenesis, and drug resistance in a more realistic setting. And these advances permit the use of personalized medicine, with 3D cultures made from patient-derived cells which are providing invaluable data, helping in the development of personalized treatment plans and in identifying how specific patients may respond to drugs [131].

Pharmaceutical and biotech companies are increasingly adopting 3D models in their research and development efforts. The FDA recognized the potential of 3D models and started to consider data from these models in the drug approval process, encouraging wider adoption across the industry [136]. Thus, in drug screening and toxicity testing, 3D cultures offer more relevant data on drug efficacy and safety, reducing the reliance on animal models and improving the translation of preclinical findings to clinical outcomes.

5. Perspectives and Conclusion Remarks

The application of nanomaterials holds tremendous potential across various domains. In the medical field, extensive research has been dedicated to exploiting their capabilities for targeted drug delivery, imaging diagnostics, photothermal therapies, and biosensors. This has led to a significant emphasis on nanoformulations as crucial drug carriers, distinguished by their capacity to improve penetration, achieve precise targeting, and enhance drug efficacy [137]. Consequently, there is a notable increase in the utilization of nanoformulations for drug screening, utilizing 3D cell culture platforms to conduct more accurate evaluations of their effects. Currently, few studies use 3D systems for drug screening due to challenges in precise evaluation and in achieving drug penetration, typically easier in monolayers. However, advancements in nanoformulation are changing this landscape.

This comprehensive review explores the intricate pharmacological landscape of compounds targeting pivotal regulators of the cell cycle and cytoskeleton, whether through direct or indirect mechanisms, showcasing a myriad of compounds with discernible cancer-specific effects. While conventional assessment of approved drugs predominantly occurs within monolayer cultures to discern clinical synergies, their indispensable role in unraveling mechanisms of resistance cannot be overstated. The utilization of 3D cell culture systems presents a paradigm shift in the landscape of preclinical drug testing, offering a multifaceted array of advantages. These include the attainment of a superior level of fidelity in mimicking in vivo conditions, amplification of cellular functionalities to a more physiologically relevant state, meticulous exploration of drug penetration dynamics and resistance mechanisms, and a laudable reduction in the reliance on animal models, aligning with ethical considerations and cost-effectiveness.

Nevertheless, the adoption of 3D culture methodologies is not devoid of challenges. The intricacies inherent in establishing and maintaining 3D cultures contribute to escalated complexities and financial burdens, while scalability issues pose formidable obstacles in the context of high-throughput screening. Furthermore, the inherent limitation in faithfully recapitulating the intricate interplay between cancer cells and the immune system, coupled with the absence of standardized protocols, underscores the imperative for continued refinement and optimization in this field of research.

Institutional Review Board Statement: Not applicable.

Informed Consent Statement: Not applicable.

Data Availability Statement: Not applicable.

Conflicts of Interest: The authors declare no conflicts of interest.

References

1. Harrison, R.G. Observations on the living developing nerve fiber. *Proc. Soc. Exp. Biol. Med.* **1906**, *4*, 140–143. [CrossRef]
2. Carrel, A. A Method for the Physiological Study of Tissues in Vitro. *J. Exp. Med.* **1923**, *38*, 407–418. [CrossRef]
3. Eagle, H. The specific amino acid requirements of a human carcinoma cell (Stain HeLa) in tissue culture. *J. Exp. Med.* **1955**, *102*, 37–48. [CrossRef]
4. Foley, G.E.; Epstein, S.S. Cell Culture and Cancer Chemotherapy. *Adv. Chemother.* **1964**, *13*, 175–353.
5. Paigen, K. The prediction of growth-inhibitory drug combinations showing enhanced differential toxicity and collateral sensitivity. *Cancer Res.* **1962**, *22*, 1290–1296.
6. Sporn, M.B. Commentary on Eagle and Foley: Cytotoxicity in Human Cell Cultures. *Cancer Res.* **2016**, *76*, 989–990. [CrossRef]
7. Gayan, S.; Teli, A.; Dey, T. Inherent aggressive character of invasive and non-invasive cells dictates the in vitro migration pattern of multicellular spheroid. *Sci. Rep.* **2017**, *7*, 11527. [CrossRef]
8. Rebelo, S.P.; Pinto, C.; Martins, T.R.; Harrer, N.; Estrada, M.F.; Loza-Alvarez, P.; Cabecadas, J.; Alves, P.M.; Gualda, E.J.; Sommergruber, W.; et al. 3D-3-culture: A tool to unveil macrophage plasticity in the tumour microenvironment. *Biomaterials* **2018**, *163*, 185–197. [CrossRef]
9. Xu, X.; Farach-Carson, M.C.; Jia, X. Three-dimensional in vitro tumor models for cancer research and drug evaluation. *Biotechnol. Adv.* **2014**, *32*, 1256–1268. [CrossRef]
10. Rose, S. A theory of the action of cancer chemotherapeutic drugs. *Clin. Exp. Immunol.* **1967**, *2*, 361–373.
11. Humtsoe, J.O.; Kramer, R.H. Differential epidermal growth factor receptor signaling regulates anchorage-independent growth by modulation of the PI3K/AKT pathway. *Oncogene* **2010**, *29*, 1214–1226. [CrossRef]
12. Huang, B.W.; Gao, J.Q. Application of 3D cultured multicellular spheroid tumor models in tumor-targeted drug delivery system research. *J. Control Release* **2018**, *270*, 246–259. [CrossRef]
13. Gharbi, S.I.; Pelletier, L.A.; Espada, A.; Gutierrez, J.; Sanfeliciano, S.M.G.; Rauch, C.T.; Ganado, M.P.; Baquero, C.; Zapatero, E.; Zhang, A.; et al. Crystal structure of active CDK4-cyclin D and mechanistic basis for abemaciclib efficacy. *NPJ Breast Cancer* **2022**, *8*, 126. [CrossRef]
14. Huang, J.; Zheng, L.; Sun, Z.; Li, J. CDK4/6 inhibitor resistance mechanisms and treatment strategies (Review). *Int. J. Mol. Med.* **2022**, *50*, 128. [CrossRef]
15. Justice, B.A.; Badr, N.A.; Felder, R.A. 3D cell culture opens new dimensions in cell-based assays. *Drug Discov. Today* **2009**, *14*, 102–107. [CrossRef]
16. Sakalem, M.E.; De Sibio, M.T.; da Costa, F.; de Oliveira, M. Historical evolution of spheroids and organoids, and possibilities of use in life sciences and medicine. *Biotechnol. J.* **2021**, *16*, e2000463. [CrossRef]
17. LaBonia, G.J.; Lockwood, S.Y.; Heller, A.A.; Spence, D.M.; Hummon, A.B. Drug penetration and metabolism in 3D cell cultures treated in a 3D printed fluidic device: Assessment of irinotecan via MALDI imaging mass spectrometry. *Proteomics* **2016**, *16*, 1814–1821. [CrossRef]
18. Hirschhaeuser, F.; Menne, H.; Dittfeld, C.; West, J.; Mueller-Klieser, W.; Kunz-Schughart, L.A. Multicellular tumor spheroids: An underestimated tool is catching up again. *J. Biotechnol.* **2010**, *148*, 3–15. [CrossRef]
19. Gozdz, A.; Wojtas, B.; Szpak, P.; Szadkowska, P.; Czernicki, T.; Marchel, A.; Wojtowicz, K.; Kaspera, W.; Ladzinski, P.; Szopa, W.; et al. Preservation of the Hypoxic Transcriptome in Glioblastoma Patient-Derived Cell Lines Maintained at Lowered Oxygen Tension. *Cancers* **2022**, *14*, 4852. [CrossRef]
20. Sant, S.; Johnston, P.A. The production of 3D tumor spheroids for cancer drug discovery. *Drug Discov. Today Technol.* **2017**, *23*, 27–36. [CrossRef]
21. Breslin, S.; O'Driscoll, L. The relevance of using 3D cell cultures, in addition to 2D monolayer cultures, when evaluating breast cancer drug sensitivity and resistance. *Oncotarget* **2016**, *7*, 45745–45756. [CrossRef]
22. Hou, S.; Tiriac, H.; Sridharan, B.P.; Scampavia, L.; Madoux, F.; Seldin, J.; Souza, G.R.; Watson, D.; Tuveson, D.; Spicer, T.P. Advanced Development of Primary Pancreatic Organoid Tumor Models for High-Throughput Phenotypic Drug Screening. *SLAS Discov.* **2018**, *23*, 574–584. [CrossRef]

23. Zhao, Y.; Tanaka, S.; Yuan, B.; Sugiyama, K.; Onda, K.; Kiyomi, A.; Takagi, N.; Sugiura, M.; Hirano, T. Arsenic Disulfide Combined with L-Buthionine-(S, R)-Sulfoximine Induces Synergistic Antitumor Effects in Two-Dimensional and Three-Dimensional Models of MCF-7 Breast Carcinoma Cells. *Am. J. Chin. Med.* **2019**, *47*, 1149–1170. [CrossRef]

24. Ryabaya, O.; Prokofieva, A.; Akasov, R.; Khochenkov, D.; Emelyanova, M.; Burov, S.; Markvicheva, E.; Inshakov, A.; Stepanova, E. Metformin increases antitumor activity of MEK inhibitor binimetinib in 2D and 3D models of human metastatic melanoma cells. *Biomed. Pharmacother.* **2019**, *109*, 2548–2560. [CrossRef]

25. Riess, C.; Koczan, D.; Schneider, B.; Linke, C.; Del Moral, K.; Classen, C.F.; Maletzki, C. Cyclin-dependent kinase inhibitors exert distinct effects on patient-derived 2D and 3D glioblastoma cell culture models. *Cell Death Discov.* **2021**, *7*, 54. [CrossRef]

26. Gulde, S.; Foscarini, A.; April-Monn, S.L.; Genio, E.; Marangelo, A.; Satam, S.; Helbling, D.; Falconi, M.; Toledo, R.A.; Schrader, J.; et al. Combined Targeting of Pathogenetic Mechanisms in Pancreatic Neuroendocrine Tumors Elicits Synergistic Antitumor Effects. *Cancers* **2022**, *14*, 5481. [CrossRef]

27. Sargenti, A.; Musmeci, F.; Cavallo, C.; Mazzeschi, M.; Bonetti, S.; Pasqua, S.; Bacchi, F.; Filardo, G.; Gazzola, D.; Lauriola, M.; et al. A new method for the study of biophysical and morphological parameters in 3D cell cultures: Evaluation in LoVo spheroids treated with crizotinib. *PLoS ONE* **2021**, *16*, e0252907. [CrossRef]

28. Van Der Steen, N.; Leonetti, A.; Keller, K.; Dekker, H.; Funel, N.; Lardon, F.; Ruijtenbeek, R.; Tiseo, M.; Rolfo, C.; Pauwels, P.; et al. Decrease in phospho-PRAS40 plays a role in the synergy between erlotinib and crizotinib in an EGFR and cMET wild-type squamous non-small cell lung cancer cell line. *Biochem. Pharmacol.* **2019**, *166*, 128–138. [CrossRef]

29. Balmana, M.; Diniz, F.; Feijao, T.; Barrias, C.C.; Mereiter, S.; Reis, C.A. Analysis of the Effect of Increased alpha2,3-Sialylation on RTK Activation in MKN45 Gastric Cancer Spheroids Treated with Crizotinib. *Int. J. Mol. Sci.* **2020**, *21*, 722. [CrossRef]

30. Lin, C.H.; Elkholy, K.H.; Wani, N.A.; Li, D.; Hu, P.; Barajas, J.M.; Yu, L.; Zhang, X.; Jacob, S.T.; Khan, W.N.; et al. Ibrutinib Potentiates Antihepatocarcinogenic Efficacy of Sorafenib by Targeting EGFR in Tumor Cells and BTK in Immune Cells in the Stroma. *Mol. Cancer Ther.* **2020**, *19*, 384–396. [CrossRef]

31. Frolov, A.; Evans, I.M.; Li, N.; Sidlauskas, K.; Paliashvili, K.; Lockwood, N.; Barrett, A.; Brandner, S.; Zachary, I.C.; Frankel, P. Imatinib and Nilotinib increase glioblastoma cell invasion via Abl-independent stimulation of p130Cas and FAK signalling. *Sci. Rep.* **2016**, *6*, 27378. [CrossRef]

32. Silveira, E.; Cavalcante, I.P.; Kremer, J.L.; de Mendonca, P.O.R.; Lotfi, C.F.P. The tyrosine kinase inhibitor nilotinib is more efficient than mitotane in decreasing cell viability in spheroids prepared from adrenocortical carcinoma cells. *Cancer Cell Int.* **2018**, *18*, 29. [CrossRef]

33. Zoetemelk, M.; Rausch, M.; Colin, D.J.; Dormond, O.; Nowak-Sliwinska, P. Short-term 3D culture systems of various complexity for treatment optimization of colorectal carcinoma. *Sci. Rep.* **2019**, *9*, 7103. [CrossRef]

34. Luan, Q.; Becker, J.H.; Macaraniag, C.; Massad, M.G.; Zhou, J.; Shimamura, T.; Papautsky, I. Non-small cell lung carcinoma spheroid models in agarose microwells for drug response studies. *Lab. Chip* **2022**, *22*, 2364–2375. [CrossRef]

35. Sabetta, S.; Vecchiotti, D.; Clementi, L.; Di Vito Nolfi, M.; Zazzeroni, F.; Angelucci, A. Comparative Analysis of Dasatinib Effect between 2D and 3D Tumor Cell Cultures. *Pharmaceutics* **2023**, *15*, 372. [CrossRef]

36. Li, Q.; Chen, C.; Kapadia, A.; Zhou, Q.; Harper, M.K.; Schaack, J.; LaBarbera, D.V. 3D models of epithelial-mesenchymal transition in breast cancer metastasis: High-throughput screening assay development, validation, and pilot screen. *J. Biomol. Screen.* **2011**, *16*, 141–154. [CrossRef]

37. Romualdo, G.R.; Da Silva, T.C.; de Albuquerque Landi, M.F.; Morais, J.A.; Barbisan, L.F.; Vinken, M.; Oliveira, C.P.; Cogliati, B. Sorafenib reduces steatosis-induced fibrogenesis in a human 3D co-culture model of non-alcoholic fatty liver disease. *Environ. Toxicol.* **2021**, *36*, 168–176. [CrossRef]

38. Cucarull, B.; Tutusaus, A.; Subias, M.; Stefanovic, M.; Hernaez-Alsina, T.; Boix, L.; Reig, M.; Garcia de Frutos, P.; Mari, M.; Colell, A.; et al. Regorafenib Alteration of the BCL-xL/MCL-1 Ratio Provides a Therapeutic Opportunity for BH3-Mimetics in Hepatocellular Carcinoma Models. *Cancers* **2020**, *12*, 332. [CrossRef]

39. Goudar, V.S.; Koduri, M.P.; Ta, Y.N.; Chen, Y.; Chu, L.A.; Lu, L.S.; Tseng, F.G. Impact of a Desmoplastic Tumor Microenvironment for Colon Cancer Drug Sensitivity: A Study with 3D Chimeric Tumor Spheroids. *ACS Appl. Mater. Interfaces* **2021**, *13*, 48478–48491. [CrossRef]

40. Bar, S.I.; Biersack, B.; Schobert, R. 3D cell cultures, as a surrogate for animal models, enhance the diagnostic value of preclinical in vitro investigations by adding information on the tumour microenvironment: A comparative study of new dual-mode HDAC inhibitors. *Investig. New Drugs* **2022**, *40*, 953–961. [CrossRef]

41. Bhagat, S.D.; Singh, U.; Mishra, R.K.; Srivastava, A. An Endogenous Reactive Oxygen Species (ROS)-Activated Histone Deacetylase Inhibitor Prodrug for Cancer Chemotherapy. *ChemMedChem* **2018**, *13*, 2073–2079. [CrossRef]

42. Robertson, F.M.; Woodward, W.A.; Pickei, R.; Ye, Z.; Bornmann, W.; Pal, A.; Peng, Z.; Hall, C.S.; Cristofanilli, M. Suberoylanilide hydroxamic acid blocks self-renewal and homotypic aggregation of inflammatory breast cancer spheroids. *Cancer* **2010**, *116*, 2760–2767. [CrossRef]

43. Godugu, C.; Patel, A.R.; Desai, U.; Andey, T.; Sams, A.; Singh, M. AlgiMatrix based 3D cell culture system as an in-vitro tumor model for anticancer studies. *PLoS ONE* **2013**, *8*, e53708. [CrossRef]

44. Li, M.; Lu, B.; Dong, X.; Zhou, Y.; He, Y.; Zhang, T.; Bao, L. Enhancement of cisplatin-induced cytotoxicity against cervical cancer spheroid cells by targeting long non-coding RNAs. *Pathol. Res. Pract.* **2019**, *215*, 152653. [CrossRef]

45. Tanenbaum, L.M.; Mantzavinou, A.; Subramanyam, K.S.; Del Carmen, M.G.; Cima, M.J. Ovarian cancer spheroid shrinkage following continuous exposure to cisplatin is a function of spheroid diameter. *Gynecol. Oncol.* **2017**, *146*, 161–169. [CrossRef]

46. Baek, N.; Seo, O.W.; Lee, J.; Hulme, J.; An, S.S. Real-time monitoring of cisplatin cytotoxicity on three-dimensional spheroid tumor cells. *Drug Des. Devel Ther.* **2016**, *10*, 2155–2165.

47. Tai, J.; Cheung, S.S.; Ou, D.; Warnock, G.L.; Hasman, D. Antiproliferation activity of Devil's club (Oplopanax horridus) and anticancer agents on human pancreatic cancer multicellular spheroids. *Phytomedicine* **2014**, *21*, 506–514. [CrossRef]

48. Johnson, P.A.; Menegatti, S.; Chambers, A.C.; Alibhai, D.; Collard, T.J.; Williams, A.C.; Bayley, H.; Perriman, A.W. A rapid high throughput bioprinted colorectal cancer spheroid platform forin vitrodrug- and radiation-response. *Biofabrication* **2022**, *15*, 014103.

49. Perche, F.; Torchilin, V.P. Cancer cell spheroids as a model to evaluate chemotherapy protocols. *Cancer Biol. Ther.* **2012**, *13*, 1205–1213. [CrossRef]

50. Eetezadi, S.; Evans, J.C.; Shen, Y.T.; De Souza, R.; Piquette-Miller, M.; Allen, C. Ratio-Dependent Synergism of a Doxorubicin and Olaparib Combination in 2D and Spheroid Models of Ovarian Cancer. *Mol. Pharm.* **2018**, *15*, 472–485. [CrossRef]

51. Gomes, A.; Russo, A.; Vidal, G.; Demange, E.; Pannetier, P.; Souguir, Z.; Lagarde, J.M.; Ducommun, B.; Lobjois, V. Evaluation by quantitative image analysis of anticancer drug activity on multicellular spheroids grown in 3D matrices. *Oncol. Lett.* **2016**, *12*, 4371–4376. [CrossRef]

52. Mellor, H.R.; Callaghan, R. Accumulation and distribution of doxorubicin in tumour spheroids: The influence of acidity and expression of P-glycoprotein. *Cancer Chemother. Pharmacol.* **2011**, *68*, 1179–1190. [CrossRef] [PubMed]

53. Ma, J.; Li, N.; Wang, Y.; Wang, L.; Wei, W.; Shen, L.; Sun, Y.; Jiao, Y.; Chen, W.; Liu, J. Engineered 3D tumour model for study of glioblastoma aggressiveness and drug evaluation on a detachably assembled microfluidic device. *Biomed. Microdevices* **2018**, *20*, 80. [CrossRef] [PubMed]

54. Weiswald, L.B.; Bellet, D.; Dangles-Marie, V. Spherical cancer models in tumor biology. *Neoplasia* **2015**, *17*, 1–15. [CrossRef] [PubMed]

55. Olive, P.L.; Durand, R.E. Drug and radiation resistance in spheroids: Cell contact and kinetics. *Cancer Metastasis Rev.* **1994**, *13*, 121–138. [CrossRef] [PubMed]

56. Goschl, S.; Schreiber-Brynzak, E.; Pichler, V.; Cseh, K.; Heffeter, P.; Jungwirth, U.; Jakupec, M.A.; Berger, W.; Keppler, B.K. Comparative studies of oxaliplatin-based platinum(iv) complexes in different in vitro and in vivo tumor models. *Metallomics* **2017**, *9*, 309–322. [CrossRef] [PubMed]

57. Fiorillo, M.; Sotgia, F.; Lisanti, M.P. "Energetic" Cancer Stem Cells (e-CSCs): A New Hyper-Metabolic and Proliferative Tumor Cell Phenotype, Driven by Mitochondrial Energy. *Front. Oncol.* **2018**, *8*, 677. [CrossRef] [PubMed]

58. Bilir, A.; Erguven, M.; Ermis, E.; Sencan, M.; Yazihan, N. Combination of imatinib mesylate with lithium chloride and medroxyprogesterone acetate is highly active in Ishikawa endometrial carcinoma in vitro. *J. Gynecol. Oncol.* **2011**, *22*, 225–232. [CrossRef] [PubMed]

59. Ek, F.; Blom, K.; Selvin, T.; Rudfeldt, J.; Andersson, C.; Senkowski, W.; Brechot, C.; Nygren, P.; Larsson, R.; Jarvius, M.; et al. Sorafenib and nitazoxanide disrupt mitochondrial function and inhibit regrowth capacity in three-dimensional models of hepatocellular and colorectal carcinoma. *Sci. Rep.* **2022**, *12*, 8943. [CrossRef] [PubMed]

60. Raimundo, L.; Paterna, A.; Calheiros, J.; Ribeiro, J.; Cardoso, D.S.P.; Piga, I.; Neto, S.J.; Hegan, D.; Glazer, P.M.; Indraccolo, S.; et al. BBIT20 inhibits homologous DNA repair with disruption of the BRCA1-BARD1 interaction in breast and ovarian cancer. *Br. J. Pharmacol.* **2021**, *178*, 3627–3647. [CrossRef]

61. Laurent, J.; Frongia, C.; Cazales, M.; Mondesert, O.; Ducommun, B.; Lobjois, V. Multicellular tumor spheroid models to explore cell cycle checkpoints in 3D. *BMC Cancer* **2013**, *13*, 73. [CrossRef] [PubMed]

62. Kwok, T.T.; Twentyman, P.R. Use of a tritiated thymidine suicide technique in the study of the cytotoxic drug response of cells located at different depths within multicellular spheroids. *Br. J. Cancer* **1987**, *55*, 367–374. [CrossRef] [PubMed]

63. Rossi, U.A.; Finocchiaro, L.M.E.; Glikin, G.C. Bortezomib Enhances the Antitumor Effects of Interferon-beta Gene Transfer on Melanoma Cells. *Anticancer Agents Med. Chem.* **2017**, *17*, 754–761. [CrossRef] [PubMed]

64. Mansoori, B.; Najafi, S.; Mohammadi, A.; AsadollahSeraj, H.; Savadi, P.; Nazari, A.; Mokhtarzadeh, A.; Roshani, E.; Duijf, P.H.; Cho, W.C.; et al. The synergy between miR-486-5p and tamoxifen causes profound cell death of tamoxifen-resistant breast cancer cells. *Biomed Pharmacother.* **2021**, *141*, 111925. [CrossRef]

65. La Monica, S.; Fumarola, C.; Cretella, D.; Bonelli, M.; Minari, R.; Cavazzoni, A.; Digiacomo, G.; Galetti, M.; Volta, F.; Mancini, M.; et al. Efficacy of the CDK4/6 Dual Inhibitor Abemaciclib in EGFR-Mutated NSCLC Cell Lines with Different Resistance Mechanisms to Osimertinib. *Cancers* **2020**, *13*, 6. [CrossRef] [PubMed]

66. Murakami, K.; Kita, Y.; Sakatani, T.; Hamada, A.; Mizuno, K.; Nakamura, K.; Takada, H.; Matsumoto, K.; Sano, T.; Goto, T.; et al. Antitumor effect of WEE1 blockade as monotherapy or in combination with cisplatin in urothelial cancer. *Cancer Sci.* **2021**, *112*, 3669–3681. [CrossRef] [PubMed]

67. Mushtaq, S.; Shahzad, K.; Saeed, T.; Ul-Hamid, A.; Abbasi, B.H.; Ahmad, N.; Khalid, W.; Atif, M.; Ali, Z.; Abbasi, R. Biocompatibility and cytotoxicity in vitro of surface-functionalized drug-loaded spinel ferrite nanoparticles. *Beilstein J. Nanotechnol.* **2021**, *12*, 1339–1364. [CrossRef]

68. Vaidya, B.; Parvathaneni, V.; Kulkarni, N.S.; Shukla, S.K.; Damon, J.K.; Sarode, A.; Kanabar, D.; Garcia, J.V.; Mitragotri, S.; Muth, A.; et al. Cyclodextrin modified erlotinib loaded PLGA nanoparticles for improved therapeutic efficacy against non-small cell lung cancer. *Int. J. Biol. Macromol.* **2019**, *122*, 338–347. [CrossRef]

69. Reddy, V.G.; Reddy, T.S.; Jadala, C.; Reddy, M.S.; Sultana, F.; Akunuri, R.; Bhargava, S.K.; Wlodkowic, D.; Srihari, P.; Kamal, A. Pyrazolo-benzothiazole hybrids: Synthesis, anticancer properties and evaluation of antiangiogenic activity using in vitro VEGFR-2 kinase and in vivo transgenic zebrafish model. *Eur. J. Med. Chem.* **2019**, *182*, 111609. [CrossRef]

70. Pandey, A.K.; Piplani, N.; Mondal, T.; Katranidis, A.; Bhattacharya, J. Efficient delivery of hydrophobic drug, Cabazitaxel, using Nanodisc: A nano sized free standing planar lipid bilayer. *J. Mol. Liq.* **2021**, *339*, 116690. [CrossRef]

71. Wu, S.; Guo, Z.; Hopkins, C.D.; Wei, N.; Chu, E.; Wipf, P.; Schmitz, J.C. Bis-cyclopropane analog of disorazole C1 is a microtubule-destabilizing agent active in ABCB1-overexpressing human colon cancer cells. *Oncotarget* **2015**, *6*, 40866–40879. [CrossRef]

72. Quinones, J.P.; Roschger, C.; Iturmendi, A.; Henke, H.; Zierer, A.; Peniche-Covas, C.; Bruggemann, O. Polyphosphazene-Based Nanocarriers for the Release of Camptothecin and Epirubicin. *Pharmaceutics* **2022**, *14*, 169. [CrossRef]

73. Croix, B.S.; Rak, J.W.; Kapitain, S.; Sheehan, C.; Graham, C.H.; Kerbel, R.S. Reversal by hyaluronidase of adhesion-dependent multicellular drug resistance in mammary carcinoma cells. *J. Natl. Cancer Inst.* **1996**, *88*, 1285–1296. [CrossRef] [PubMed]

74. Rae, C.; Mairs, R.J. Evaluation of the radiosensitizing potency of chemotherapeutic agents in prostate cancer cells. *Int. J. Radiat. Biol.* **2017**, *93*, 194–203. [CrossRef]

75. Sexton, R.; Mahdi, Z.; Chaudhury, R.; Beydoun, R.; Aboukameel, A.; Khan, H.Y.; Baloglu, E.; Senapedis, W.; Landesman, Y.; Tesfaye, A.; et al. Targeting Nuclear Exporter Protein XPO1/CRM1 in Gastric Cancer. *Int. J. Mol. Sci.* **2019**, *20*, 4826. [CrossRef]

76. Daphu, I.; Horn, S.; Stieber, D.; Varughese, J.K.; Spriet, E.; Dale, H.A.; Skaftnesmo, K.O.; Bjerkvig, R.; Thorsen, F. In vitro treatment of melanoma brain metastasis by simultaneously targeting the MAPK and PI3K signaling pathways. *Int. J. Mol. Sci.* **2014**, *15*, 8773–8794. [CrossRef] [PubMed]

77. Tang, J.H.; Yang, L.; Chen, J.X.; Li, Q.R.; Zhu, L.R.; Xu, Q.F.; Huang, G.H.; Zhang, Z.X.; Xiang, Y.; Du, L.; et al. Bortezomib inhibits growth and sensitizes glioma to temozolomide (TMZ) via down-regulating the FOXM1-Survivin axis. *Cancer Commun.* **2019**, *39*, 81. [CrossRef]

78. Nilubol, N.; Boufraqech, M.; Zhang, L.; Gaskins, K.; Shen, M.; Zhang, Y.Q.; Gara, S.K.; Austin, C.P.; Kebebew, E. Synergistic combination of flavopiridol and carfilzomib targets commonly dysregulated pathways in adrenocortical carcinoma and has biomarkers of response. *Oncotarget* **2018**, *9*, 33030–33042. [CrossRef] [PubMed]

79. Bellat, V.; Verchere, A.; Ashe, S.A.; Law, B. Transcriptomic insight into salinomycin mechanisms in breast cancer cell lines: Synergistic effects with dasatinib and induction of estrogen receptor beta. *BMC Cancer* **2020**, *20*, 661. [CrossRef]

80. Kretschmer, I.; Freudenberger, T.; Twarock, S.; Fischer, J.W. Synergistic effect of targeting the epidermal growth factor receptor and hyaluronan synthesis in oesophageal squamous cell carcinoma cells. *Br. J. Pharmacol.* **2015**, *172*, 4560–4574. [CrossRef]

81. Acikgoz, E.; Guven, U.; Duzagac, F.; Uslu, R.; Kara, M.; Soner, B.C.; Oktem, G. Enhanced G2/M Arrest, Caspase Related Apoptosis and Reduced E-Cadherin Dependent Intercellular Adhesion by Trabectedin in Prostate Cancer Stem Cells. *PLoS ONE* **2015**, *10*, e0141090. [CrossRef]

82. Schneider, N.F.Z.; Menegaz, D.; Dagostin, A.L.A.; Persich, L.; Rocha, S.C.; Ramos, A.C.P.; Cortes, V.F.; Fontes, C.F.L.; de Padua, R.M.; Munkert, J.; et al. Cytotoxicity of glucoevatromonoside alone and in combination with chemotherapy drugs and their effects on Na(+),K(+)-ATPase and ion channels on lung cancer cells. *Mol. Cell Biochem.* **2021**, *476*, 1825–1848. [CrossRef]

83. MacDonald, J.; Ramos-Valdes, Y.; Perampalam, P.; Litovchick, L.; DiMattia, G.E.; Dick, F.A. A Systematic Analysis of Negative Growth Control Implicates the DREAM Complex in Cancer Cell Dormancy. *Mol. Cancer Res.* **2017**, *15*, 371–381. [CrossRef]

84. Balahmar, R.M.; Deepak, V.; Sivasubramaniam, S. Doxorubicin resistant choriocarcinoma cell line derived spheroidal cells exhibit stem cell markers but reduced invasion. *3 Biotech.* **2022**, *12*, 184. [CrossRef] [PubMed]

85. Crews, C.M.; Erikson, R.L. Extracellular signals and reversible protein phosphorylation: What to Mek of it all. *Cell* **1993**, *74*, 215–217. [CrossRef]

86. Morelli, M.P.; Tentler, J.J.; Kulikowski, G.N.; Tan, A.C.; Bradshaw-Pierce, E.L.; Pitts, T.M.; Brown, A.M.; Nallapareddy, S.; Arcaroli, J.J.; Serkova, N.J.; et al. Preclinical activity of the rational combination of selumetinib (AZD6244) in combination with vorinostat in KRAS-mutant colorectal cancer models. *Clin. Cancer Res.* **2012**, *18*, 1051–1062. [CrossRef]

87. Ogishima, J.; Taguchi, A.; Kawata, A.; Kawana, K.; Yoshida, M.; Yoshimatsu, Y.; Sato, M.; Nakamura, H.; Kawata, Y.; Nishijima, A.; et al. The oncogene KRAS promotes cancer cell dissemination by stabilizing spheroid formation via the MEK pathway. *BMC Cancer* **2018**, *18*, 1201. [CrossRef] [PubMed]

88. Cagle, P.; Niture, S.; Srivastava, A.; Ramalinga, M.; Aqeel, R.; Rios-Colon, L.; Chimeh, U.; Suy, S.; Collins, S.P.; Dahiya, R.; et al. MicroRNA-214 targets PTK6 to inhibit tumorigenic potential and increase drug sensitivity of prostate cancer cells. *Sci. Rep.* **2019**, *9*, 9776. [CrossRef] [PubMed]

89. Azmi, A.S.; Khan, H.Y.; Muqbil, I.; Aboukameel, A.; Neggers, J.E.; Daelemans, D.; Mahipal, A.; Dyson, G.; Kamgar, M.; Al-Hallak, M.N.; et al. Preclinical Assessment with Clinical Validation of Selinexor with Gemcitabine and Nab-Paclitaxel for the Treatment of Pancreatic Ductal Adenocarcinoma. *Clin. Cancer Res.* **2020**, *26*, 1338–1348. [CrossRef]

90. Liu, S.; Cheng, H.; Kwan, W.; Lubieniecka, J.M.; Nielsen, T.O. Histone deacetylase inhibitors induce growth arrest, apoptosis, and differentiation in clear cell sarcoma models. *Mol. Cancer Ther.* **2008**, *7*, 1751–1761. [CrossRef]

91. L'Esperance, S.; Bachvarova, M.; Tetu, B.; Mes-Masson, A.M.; Bachvarov, D. Global gene expression analysis of early response to chemotherapy treatment in ovarian cancer spheroids. *BMC Genom.* **2008**, *9*, 99. [CrossRef] [PubMed]

92. Pollard, T.D.; Goldman, R.D. Overview of the Cytoskeleton from an Evolutionary Perspective. *Cold Spring Harb. Perspect. Biol.* **2018**, *10*, a030288. [CrossRef]

93. Fletcher, D.A.; Mullins, R.D. Cell mechanics and the cytoskeleton. *Nature* **2010**, *463*, 485–492. [CrossRef]

94. Hohmann, T.; Dehghani, F. The Cytoskeleton-A Complex Interacting Meshwork. *Cells* **2019**, *8*, 362. [CrossRef]
95. Pollard, T.D.; Borisy, G.G. Cellular motility driven by assembly and disassembly of actin filaments. *Cell* **2003**, *112*, 453–465. [CrossRef] [PubMed]
96. Flitney, E.W.; Kuczmarski, E.R.; Adam, S.A.; Goldman, R.D. Insights into the mechanical properties of epithelial cells: The effects of shear stress on the assembly and remodeling of keratin intermediate filaments. *FASEB J.* **2009**, *23*, 2110–2119. [CrossRef]
97. van Vuuren, R.J.; Visagie, M.H.; Theron, A.E.; Joubert, A.M. Antimitotic drugs in the treatment of cancer. *Cancer Chemother. Pharmacol.* **2015**, *76*, 1101–1112. [CrossRef]
98. Field, J.J.; Diaz, J.F.; Miller, J.H. The binding sites of microtubule-stabilizing agents. *Chem. Biol.* **2013**, *20*, 301–315. [CrossRef] [PubMed]
99. Rohena, C.C.; Mooberry, S.L. Recent progress with microtubule stabilizers: New compounds, binding modes and cellular activities. *Nat. Prod. Rep.* **2014**, *31*, 335–355. [CrossRef]
100. Dumontet, C.; Jordan, M.A. Microtubule-binding agents: A dynamic field of cancer therapeutics. *Nat. Rev. Drug Discov.* **2010**, *9*, 790–803. [CrossRef]
101. Gandalovicova, A.; Rosel, D.; Fernandes, M.; Vesely, P.; Heneberg, P.; Cermak, V.; Petruzelka, L.; Kumar, S.; Sanz-Moreno, V.; Brabek, J. Migrastatics-Anti-metastatic and Anti-invasion Drugs: Promises and Challenges. *Trends Cancer* **2017**, *3*, 391–406. [CrossRef] [PubMed]
102. Allingham, J.S.; Klenchin, V.A.; Rayment, I. Actin-targeting natural products: Structures, properties and mechanisms of action. *Cell Mol. Life Sci.* **2006**, *63*, 2119–2134. [CrossRef] [PubMed]
103. Wang, S.; Crevenna, A.H.; Ugur, I.; Marion, A.; Antes, I.; Kazmaier, U.; Hoyer, M.; Lamb, D.C.; Gegenfurtner, F.; Kliesmete, Z.; et al. Actin stabilizing compounds show specific biological effects due to their binding mode. *Sci. Rep.* **2019**, *9*, 9731. [CrossRef] [PubMed]
104. Fenteany, G.; Zhu, S. Small-molecule inhibitors of actin dynamics and cell motility. *Curr. Top. Med. Chem.* **2003**, *3*, 593–616. [CrossRef] [PubMed]
105. Johnson-Arbor, K.; Dubey, R. *Doxorubicin*; StatPearls Publishing LLC: Treasure Island, FL, USA, 2023.
106. Zhang, Y.; Li, K.; Han, X.; Chen, Q.; Shao, L.; Bai, D. A photochemical-responsive nanoparticle boosts doxorubicin uptake to suppress breast cancer cell proliferation by apoptosis. *Sci. Rep.* **2022**, *12*, 10354. [CrossRef] [PubMed]
107. Ahmed, H.; Ajat, M.; Mahmood, R.I.; Mansor, R.; Razak, I.S.A.; Al-Obaidi, J.R.; Razali, N.; Jaji, A.Z.; Danmaigoro, A.; Bakar, M.Z.A. LC-MS/MS Proteomic Study of MCF-7 Cell Treated with Dox and Dox-Loaded Calcium Carbonate Nanoparticles Revealed Changes in Proteins Related to Glycolysis, Actin Signalling, and Energy Metabolism. *Biology* **2021**, *10*, 909. [CrossRef] [PubMed]
108. Koczurkiewicz-Adamczyk, P.; Piska, K.; Gunia-Krzyzak, A.; Bucki, A.; Jamrozik, M.; Lorenc, E.; Ryszawy, D.; Wojcik-Pszczola, K.; Michalik, M.; Marona, H.; et al. Cinnamic acid derivatives as chemosensitising agents against DOX-treated lung cancer cells—Involvement of carbonyl reductase 1. *Eur. J. Pharm. Sci.* **2020**, *154*, 105511. [CrossRef] [PubMed]
109. Ma, L.; Liu, Y.P.; Geng, C.Z.; Xing, L.X.; Zhang, X.H. Low-dose epirubicin inhibits ezrin-mediated metastatic behavior of breast cancer cells. *Tumori* **2011**, *97*, 400–405. [CrossRef] [PubMed]
110. Lipreri da Silva, J.C.; Vicari, H.P.; Machado-Neto, J.A. Perspectives for Targeting Ezrin in Cancer Development and Progression. *Future Pharmacol.* **2023**, *3*, 61–79. [CrossRef]
111. Kozminski, P.; Halik, P.K.; Chesori, R.; Gniazdowska, E. Overview of Dual-Acting Drug Methotrexate in Different Neurological Diseases, Autoimmune Pathologies and Cancers. *Int. J. Mol. Sci.* **2020**, *21*, 3483. [CrossRef]
112. Mazur, A.J.; Nowak, D.; Mannherz, H.G.; Malicka-Blaszkiewicz, M. Methotrexate induces apoptosis in CaSki and NRK cells and influences the organization of their actin cytoskeleton. *Eur. J. Pharmacol.* **2009**, *613*, 24–33. [CrossRef] [PubMed]
113. Ku, H.C.; Cheng, C.F. Master Regulator Activating Transcription Factor 3 (ATF3) in Metabolic Homeostasis and Cancer. *Front. Endocrinol.* **2020**, *11*, 556. [CrossRef] [PubMed]
114. Ohtsubo, H.; Okada, T.; Nozu, K.; Takaoka, Y.; Shono, A.; Asanuma, K.; Zhang, L.; Nakanishi, K.; Taniguchi-Ikeda, M.; Kaito, H.; et al. Identification of mutations in FN1 leading to glomerulopathy with fibronectin deposits. *Pediatr. Nephrol.* **2016**, *31*, 1459–1467. [CrossRef] [PubMed]
115. Wang, H.; Guo, S.; Kim, S.J.; Shao, F.; Ho, J.W.K.; Wong, K.U.; Miao, Z.; Hao, D.; Zhao, M.; Xu, J.; et al. Cisplatin prevents breast cancer metastasis through blocking early EMT and retards cancer growth together with paclitaxel. *Theranostics* **2021**, *11*, 2442–2459. [CrossRef] [PubMed]
116. Wang, X.; Tanaka, M.; Krstin, S.; Peixoto, H.S.; Moura, C.C.M.; Wink, M. Cytoskeletal interference—A new mode of action for the anticancer drugs camptothecin and topotecan. *Eur. J. Pharmacol.* **2016**, *789*, 265–274. [CrossRef] [PubMed]
117. Kang, E.; Seo, J.; Yoon, H.; Cho, S. The Post-Translational Regulation of Epithelial-Mesenchymal Transition-Inducing Transcription Factors in Cancer Metastasis. *Int. J. Mol. Sci.* **2021**, *22*, 3591. [CrossRef] [PubMed]
118. Li, Y.; Zhang, X.; Yang, Z.; Han, B.; Chen, L.A. miR-339-5p inhibits metastasis of non-small cell lung cancer by regulating the epithelial-to-mesenchymal transition. *Oncol. Lett.* **2018**, *15*, 2508–2514. [CrossRef] [PubMed]
119. Bhullar, K.S.; Lagaron, N.O.; McGowan, E.M.; Parmar, I.; Jha, A.; Hubbard, B.P.; Rupasinghe, H.P.V. Kinase-targeted cancer therapies: Progress, challenges and future directions. *Mol. Cancer* **2018**, *17*, 48. [CrossRef] [PubMed]
120. Iqbal, N. Imatinib: A breakthrough of targeted therapy in cancer. *Chemother. Res. Pract.* **2014**, *2014*, 357027. [CrossRef]

121. Popow-Wozniak, A.; Wozniakowska, A.; Kaczmarek, L.; Malicka-Blaszkiewicz, M.; Nowak, D. Apoptotic effect of imatinib on human colon adenocarcinoma cells: Influence on actin cytoskeleton organization and cell migration. *Eur. J. Pharmacol.* **2011**, *667*, 66–73. [CrossRef]

122. Ayati, A.; Moghimi, S.; Salarinejad, S.; Safavi, M.; Pouramiri, B.; Foroumadi, A. A review on progression of epidermal growth factor receptor (EGFR) inhibitors as an efficient approach in cancer targeted therapy. *Bioorg. Chem.* **2020**, *99*, 103811. [CrossRef] [PubMed]

123. Fichter, C.D.; Gudernatsch, V.; Przypadlo, C.M.; Follo, M.; Schmidt, G.; Werner, M.; Lassmann, S. ErbB targeting inhibitors repress cell migration of esophageal squamous cell carcinoma and adenocarcinoma cells by distinct signaling pathways. *J. Mol. Med.* **2014**, *92*, 1209–1223. [CrossRef] [PubMed]

124. Liu, C.; Wang, Z.; Liu, Q.; Wu, G.; Chu, C.; Li, L.; An, L.; Duan, S. Sensitivity analysis of EGFR L861Q mutation to six tyrosine kinase inhibitors. *Clin. Transl. Oncol.* **2022**, *24*, 1975–1985. [CrossRef] [PubMed]

125. Lee, H.K.; Noh, M.H.; Hong, S.W.; Kim, S.M.; Kim, S.H.; Kim, Y.S.; Broaddus, V.C.; Hur, D.Y. Erlotinib Activates Different Cell Death Pathways in EGFR-mutant Lung Cancer Cells Grown in 3D Versus 2D Culture Systems. *Anticancer. Res.* **2021**, *41*, 1261–1269. [CrossRef] [PubMed]

126. Xu, W.S.; Parmigiani, R.B.; Marks, P.A. Histone deacetylase inhibitors: Molecular mechanisms of action. *Oncogene* **2007**, *26*, 5541–5552. [CrossRef] [PubMed]

127. Iancu-Rubin, C.; Gajzer, D.; Mosoyan, G.; Feller, F.; Mascarenhas, J.; Hoffman, R. Panobinostat (LBH589)-induced acetylation of tubulin impairs megakaryocyte maturation and platelet formation. *Exp. Hematol.* **2012**, *40*, 564–574. [CrossRef] [PubMed]

128. Perez, T.; Berges, R.; Maccario, H.; Oddoux, S.; Honore, S. Low concentrations of vorinostat decrease EB1 expression in GBM cells and affect microtubule dynamics, cell survival and migration. *Oncotarget* **2021**, *12*, 304–315. [CrossRef] [PubMed]

129. Cui, X.; Hartanto, Y.; Zhang, H. Advances in multicellular spheroids formation. *J. R. Soc. Interface* **2017**, *14*, 20160877. [CrossRef]

130. Smyrek, I.; Mathew, B.; Fischer, S.C.; Lissek, S.M.; Becker, S.; Stelzer, E.H.K. E-cadherin, actin, microtubules and FAK dominate different spheroid formation phases and important elements of tissue integrity. *Biol. Open* **2019**, *8*, bio037051. [CrossRef]

131. Langhans, S.A. Three-Dimensional in Vitro Cell Culture Models in Drug Discovery and Drug Repositioning. *Front. Pharmacol.* **2018**, *9*, 6. [CrossRef]

132. Kaur, P.; Ward, B.; Saha, B.; Young, L.; Groshen, S.; Techy, G.; Lu, Y.; Atkinson, R.; Taylor, C.R.; Ingram, M.; et al. Human breast cancer histoid: An in vitro 3-dimensional co-culture model that mimics breast cancer tissue. *J. Histochem. Cytochem.* **2011**, *59*, 1087–1100. [CrossRef] [PubMed]

133. Fukuda, J.; Khademhosseini, A.; Yeo, Y.; Yang, X.; Yeh, J.; Eng, G.; Blumling, J.; Wang, C.F.; Kohane, D.S.; Langer, R. Micromolding of photocrosslinkable chitosan hydrogel for spheroid microarray and co-cultures. *Biomaterials* **2006**, *27*, 5259–5267. [CrossRef] [PubMed]

134. Lotsberg, M.L.; Rosland, G.V.; Rayford, A.J.; Dyrstad, S.E.; Ekanger, C.T.; Lu, N.; Frantz, K.; Stuhr, L.E.B.; Ditzel, H.J.; Thiery, J.P.; et al. Intrinsic Differences in Spatiotemporal Organization and Stromal Cell Interactions Between Isogenic Lung Cancer Cells of Epithelial and Mesenchymal Phenotypes Revealed by High-Dimensional Single-Cell Analysis of Heterotypic 3D Spheroid Models. *Front. Oncol.* **2022**, *12*, 818437. [CrossRef] [PubMed]

135. Lawrenson, K.; Grun, B.; Benjamin, E.; Jacobs, I.J.; Dafou, D.; Gayther, S.A. Senescent fibroblasts promote neoplastic transformation of partially transformed ovarian epithelial cells in a three-dimensional model of early stage ovarian cancer. *Neoplasia* **2010**, *12*, 317–325. [CrossRef] [PubMed]

136. Wang, H.; Brown, P.C.; Chow, E.C.Y.; Ewart, L.; Ferguson, S.S.; Fitzpatrick, S.; Freedman, B.S.; Guo, G.L.; Hedrich, W.; Heyward, S.; et al. 3D cell culture models: Drug pharmacokinetics, safety assessment, and regulatory consideration. *Clin. Transl. Sci.* **2021**, *14*, 1659–1680. [CrossRef]

137. Bottger, R.; Pauli, G.; Chao, P.H.; Al Fayez, N.; Hohenwarter, L.; Li, S.D. Lipid-based nanoparticle technologies for liver targeting. *Adv. Drug Deliv. Rev.* **2020**, *154–155*, 79–101. [CrossRef]